



## Expected Performance of CALET

K.KASAHARA<sup>1</sup>, S.TORII<sup>1</sup>, Y.SHIMIZU<sup>1</sup>, Y.AKAIKE<sup>1</sup>, K.TAIRA<sup>1</sup>, K.YOSHIDA<sup>2</sup> AND I.WATANABE<sup>2</sup>:  
FOR THE CALET COLLABORATION

<sup>1</sup>Research Inst. for Science and Engineering, Waseda Univ., Tokyo, Japan

<sup>2</sup>Shibaura Inst. of Technology, Saitama, Japan

kasahara@icrr.u-tokyo.ac.jp

**Abstract:** CALET is a detector planned to be on board ISS to investigate high energy universe by observing high energy gamma-rays, electrons and other cosmic ray. It is now in the phase A/B study period of the JAXA program. The performance of CALET was studied earlier[1] but the design structure (mainly its size) has been changed since that time. We have been performing new M.C simulations corresponding to the new structure to evaluate its basic performance. This is to report some of the new results.

## Introduction

As described in an accompanying paper[2] of this conference, CALET is a versatile detector for exploring high energy universe by observing gamma rays ( $> 20$  MeV), electrons ( $> \text{GeV}$ ) and other charged particles ( $> 100$  GeV). It is planned to be on board the JEM (Japanese Experiment Module, Kibo) of the International Space Station. Its phase A/B study has recently started as a Japan Aerospace Exploration Agency (JAXA) program. We study its basic performance by M.C simulations. They are: effective area, energy resolution, electron/proton separation.

## Structure of CALET

Figure 1 shows essential ingredients of CALET and charged particle tracks of simulated typical showers incident on it.

More than two third of the main body is covered by a plastic scintillator array which serves as an anti-coincidence detector (ACD) for low energy photon observation.

There are two layers of Si arrays with 1 cm square pixel to obtain high charge resolution of heavy particles.

Then, IMC (Imaging Calorimeter) comes. One set of IMC component consists of one thin tung-

sten plate and 2 orthogonally directed SciFi (scintillating fiber) sheets for  $x$  and  $y$  position measurement. (Single SciFi has a dimension of  $1 \text{ mm} \times 1 \text{ mm} \times 90 \text{ cm}$ .) We denote such a set by  $W_t + \text{SciFi}$  where  $t$  means the thickness of the tungsten plate in cm. Then, from top to bottom, IMC reads SciFi +  $10 \times (W_{0.027} + \text{SciFi}) + 5 \times (W_{0.062} + \text{SciFi}) + 2 \times (W_{0.338} + \text{SciFi})$ . When supporting material is included, their respective thickness is: 1, 1 and 2 radiation lengths ( $r.l$ ). The total thickness is thus  $4 r.l$  or  $0.14$  nuclear interaction mean free path ( $mfp$ ). IMC is used to know shower development profile as well as energy deposit there for energy determination.

Under IMC is put TASC (Total absorption calorimeter) consisting of a number of BGO logs, each of which has a dimension of  $30 \text{ cm} \times 2.5 \text{ cm} \times 2.5 \text{ cm}$ . TASC is composed of 4 blocks; each block is a cubic tower consisting of 12 log layers alternately aligned  $x$  and  $y$  directions. Besides energy measurement, with its position sensitiveness, TASC offers shower development profile which is essential for  $e/p$  separation.

The total thickness of TASC is  $27 r.l$  or  $1.4 mfp$ .

## Simulation conditions

We use Epics for simulation[3]. An isotropic incident particles are assumed; the zenith angle distri-

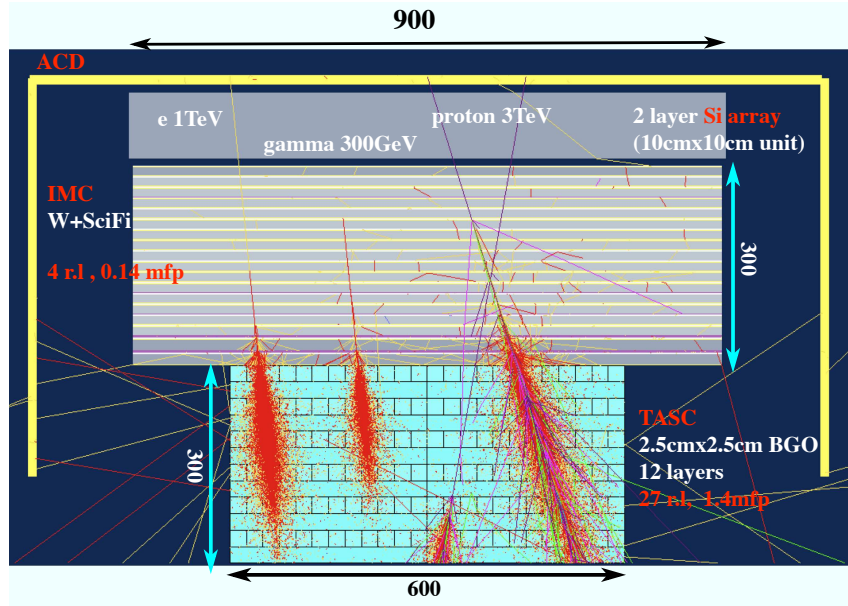


Figure 1: Schematic view of CALET and typical high energy showers. The leftmost one is a shower by a 1 TeV electron—this example starts cascading at a rather deeper position than standard ones. The next one is by a 300 GeV gamma ray which can be discriminated from electron by absence of tracks at the upper part. Next two are by 3 TeV protons which could be the main background source for electron identification.

bution is take to be  $\cos\theta d\cos\theta$  on the top surface of the detector where particles are distributed uniformly.

We assume two geometrical cases:

- “better geometry”: Incident particles are distributed on 120 cm square area with a maximum zenith angle of  $\cos\theta = 0.7$ . We select showers of which the axis is fully contained in both IMC and TASC. The exit point of the shower axis must be 2.5 cm or more apart from the edge. A minimum of 3 IMC layers must give signals along the shower axis.
- “good geometry”: The input area is a 280 cm square. A larger maximum zenith angle ( $\theta = 70^\circ$ ). We select those showers that a minimum of 3 IMC layers give signals along the shower axis, and the axis length in TASC is more than 30 cm.

## Event selection

Event selection is dependent on the trigger mode. For low energy gamma/electron observation, enormous number of protons must be rejected without serious loss of objective particles. Figure 2 shows distributions of energy deposit in the top BGO layers ( $\Delta E_{BGO}$ ) by 10 GeV electrons, gamma-rays and protons for “good geometry”. From this figure, we see that if we impose a trigger threshold to be  $\Delta E_{BGO} > 1.47$  GeV, we will be able to observe 88% of electrons, 91% of gamma-rays while rejecting 97.8% of protons (see also Table 1 which summarizes values for other conditions, too).

## Results for electron/gamma-ray

Below 10 GeV, we assume a trigger condition with  $\Delta E_{BGO}$  at 1 GeV. This naturally triggers higher energy showers but actual observation will use a separate trigger with  $\Delta E_{BGO}$  at 10 GeV. We show results by these two conditions. How-

Table 1:  $\Delta E_{BGO}$  threshold vs acceptance

geom	$E$	$\Delta E_{BGO}$	acceptance (%)		
	(GeV)		$\gamma$	e	p
better	1	0.116	96.8	95	7.9
	10	1.47	89.5	95	1.5
good	1	0.116	80.4	85.9	7.8
	10	1.47	90.6	88.4	2.2

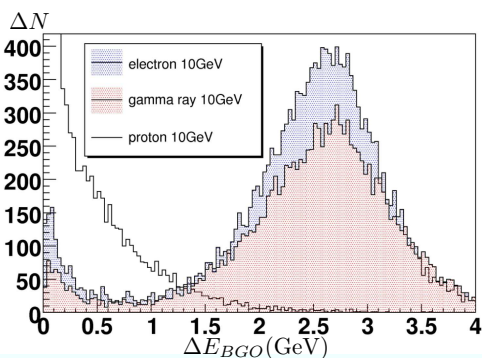


Figure 2: Energy deposit in the top BGO by 10 GeV particles

ever, for low energy gamma-ray observation, we drop the  $\Delta E_{BGO}$  condition and impose ACD anti-coincidence.

We show the results for “good geometry”.

### Effective $S\Omega$

Figure 3 shows the effective area as a function of energy for electrons.  $S\Omega \sim 7000 \text{ cm}^2\text{-sr}$  means we will be able to observe  $\sim 2000$  electrons in the TeV region with a few year exposure. Similar one for gamma-rays is shown in Fig.4. Decreasing  $S\Omega$  over 1 GeV is due to triggering of ACD by backscattered particles. There should be a possibility that we switch on ACD only below few GeV.

### Energy resolution

The r.m.s energy resolution in % is shown in Fig. 5. We note the energy resolution over 100 GeV is excellent ( better than 2%). This is important because, if a gamma line from dark matter annihila-

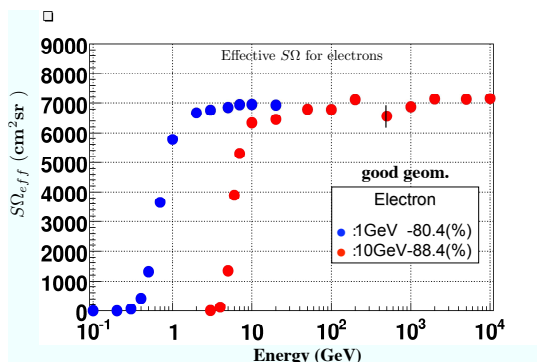


Figure 3: Effective  $S\Omega$  as a function of electron energy. Left one is for low energy trigger and right one for high energy trigger

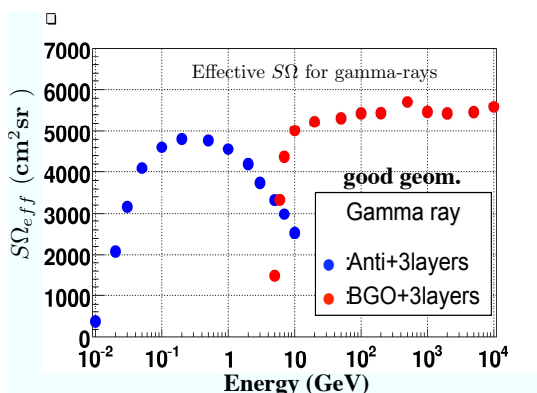


Figure 4: Effective  $S\Omega$  for gamma-rays

tion should exist, most probable energy is expected to be in this region.

### Result for protons and heavy ions

We use “better geometry” since we need the Si array for charge identification. Using the same trigger conditions as the one for high energy electrons leads to selecting events of which the first interaction takes place above the first BGO layer. Statistics are not yet enough.

### Effective $S\Omega$

The effective  $S\Omega$  is computed for proton, N, and Fe. Heavier ions naturally give higher  $S\Omega$  as seen in Fig.6 owing to larger interaction cross-sections.

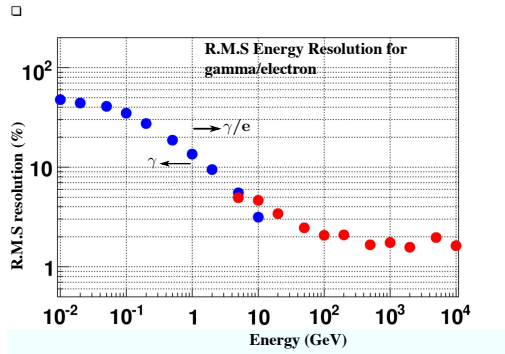


Figure 5: R.M.S energy resolution for gamma-rays and electrons. Both are essentially the same so that the gamma-ray case is show here (for electrons only  $E > 1$  GeV should be used).

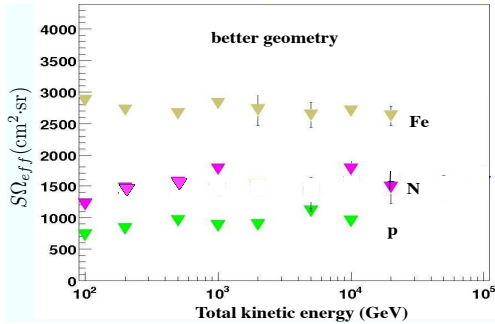


Figure 6: Effective  $S\Omega$  for p, N and Fe.

### Energy resolution

For protons, we get almost constant resolution of  $\sim 30\%$ . Heavy ions give better resolutions than proton at relatively low energies; this is due to the statistical effect. At higher energies where leakage plays an important role, the resolution approaches to  $\sim 30\%$  (Fig.7).

### e/p separation

For TeV region electron observation, excellent e/p separation is mandatory. For protons interacted in IMC, we use a diagram shown in Fig.8 where we plot energy weighted r.m.s spread of the shower at the bottom of BGO vs. the ratio of energy at the bottom BGO to the total deposited energy. A million of protons  $\geq 1$  TeV are put and those are selected which give similar energy deposit as 1

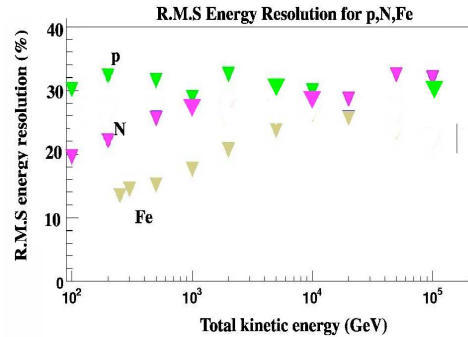


Figure 7: R.M.S energy resolution for p, N and Fe.

TeV electrons. There is no protons below the line ( $Fraction = 0.12Spread^{-2.5}$ ) in the figure. The proton rejection power in this case is  $\sim 1.5 \times 10^5$  (with some small loss of electrons).

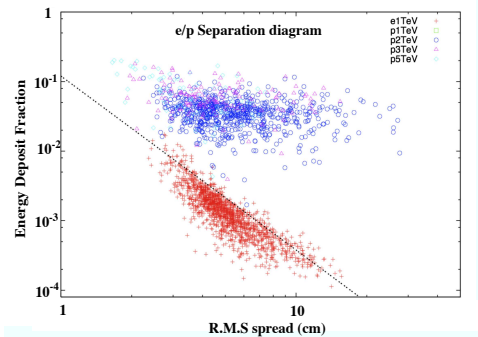


Figure 8: e/p separation diagram. The lower group is electrons and upper one protons. See text

### Summary

The CALET performance was previously studied [1]. Since then, the design structure has been changed. We could update/verify previous results. The performance matches our requirement.

### References

- [1] Chang et al., Proc. 29th ICRC, OG1.5 Vol.3(2005) 273. Proc. 28th ICRC, Vol.4 (2003) 2185
- [2] S. Torii et al. OG1.5 645: This conference.
- [3] <http://cosmos.n.kanagawa-u.ac.jp/>.